Lewis Acid Coordination Complexes of Polymers. 1. BCl_3, $AlCl_3$, and $GaCl_3$ Complexes of Poly(*p*-phenylenebenzobisthiazole)

Michael F. Roberts and Samson A. Jenekhe*

Department of Chemical Engineering and Center for Photoinduced Charge Transfer, University of Rochester, Rochester, New York 14627-0166

Received July 13, 1993®

Complexes of the rigid-rod polymer poly(*p*-phenylenebenzobisthiazole) (PBZT) with the Lewis acids BCl_3, $AlCl_3$, and $GaCl_3$ have been prepared, and their structures and properties are characterized. The complexes prepared by simultaneous complexation and solubilization in nitromethane and those prepared by complexation without solubilization in dichloromethane are shown to be identical. Complexation is found to occur by Lewis acid coordination of the sulfur and nitrogen heteroatoms of PBZT and the resultant complexes are of rigid-rod conformation in solution and have conjugated structures similar to the pure polymer. The solid $AlCl_3$ and $GaCl_3$ complexes are stable to 100 and 200 °C in nitrogen, respectively. The PBZT/$GaCl_3$ complex exhibits a glass transition at about 26 °C with an activation energy of 32 kcal/mol determined by differential scanning calorimetry and dynamic mechanical analysis. The Lewis acid coordination complexes of the conjugated rigid-rod polymer PBZT are important derivatives that facilitate elucidation of its structural, chemical, and physical properties as well as intermediates for facile processing of the pure polymer into films, coatings, fibers, and composites.

Introduction

Poly(*p*-phenylenebenzobisthiazole) (PBZT) is a conjugated rigid-rod polymer, first synthesized over 15 years ago[1] in efforts to obtain thermally and oxidatively stable materials. It has since received considerable attention because of its diverse, potentially useful properties[2-12] although it has not yet been commercialized. These include excellent mechanical properties; tensile moduli of 240 and 300 GPa and strengths of 1.5 and 3 GPa have been achieved for films[4a] and fibers,[4b] respectively, making it comparable to commercial carbon fibers and steel, although its compressive properties are not quite as impressive.[5] A theoretical upper limit of 605 GPa has been predicted for the tensile modulus.[6] PBZT exhibits excellent thermooxidative stability,[2] retaining its mechanical properties to ~650 °C and shows good chemical resistance to solvents and strong acids.[7] It has also been used as the reinforcing component in molecular composites.[3] The electroactive and optical properties of PBZT have been of interest because of its conjugated structure. Electrochemically doped samples[8] were produced with an electrical conductivity of 20 Ω^{-1} cm^{-1}. We have investigated the frequency dependent third-order nonlinear optical susceptibility $\chi^{(3)}(-3\omega;\omega,\omega,\omega)$ of PBZT films and it was found to be in the range 10^{-11}–10^{-10} esu in the spectral range 0.9–2.4 μm[9].

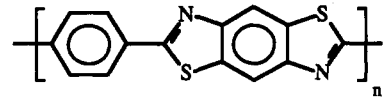

PBZT

Unfortunately, the physical properties attainable in PBZT are accompanied by extreme intractability of the polymer. In a following paper[10] we will present calculations of the intermolecular and intramolecular forces in PBZT. We find that the polymer has a rigid rodlike conformation with very efficient packing of the chains and strong intermolecular van der Waals forces. Similar conclusions were reached by others in earlier work.[11-13] Thus, the excellent mechanical properties achieved in PBZT can be traced to strong intramolecular and intermolecular forces. These same attributes, however, eliminate the possibility of melt processing (PBZT shows no discernible glass transition or melting point below its decomposition temperature of 700 °C in nitrogen) and available solvents have been limited to strong acids such as methanesulfonic

* To whom correspondence should be addressed.

® Abstract published in *Advance ACS Abstracts*, November 1, 1993.

(1) (a) Wolfe, J. F.; Loo, B. H.; Arnold, F. E. *Polym. Prepr. (Am. Chem. Soc., Polym. Chem. Div.)* **1977**, *19* (2), 1. (b) Wolfe, J. F.; Loo, B. H.; Arnold, F. E. *Macromolecules* **1981**, *14*, 915–924.

(2) Wolfe, J. F. In *Encyclopedia of Polymer Science and Engineering*, 2nd ed.; Wiley: New York, 1988; Vol. 11, pp 601–635.

(3) Adams, W. W., Eby, R. K., McLemore, D., Eds.; *The Materials Science and Engineering of Rigid-Rod Polymers*; The Materials Research Society: Pittsburgh, PA, 1989; Vol. 134.

(4) (a) Feldman, L.; Farris, R. J.; Thomas, E. L. *J. Mater. Sci.* **1985**, *20*, 2719–2726. (b) Allen, S. R.; Farris, R. J.; Thomas, E. L. *J. Mater. Sci.* **1985**, *20*, 2727–2734.

(5) DeTeresa, S. J.; Allen, S. R.; Farris, R. J. In *Composite Applications. The Role of Matrix, Fiber and Interface*; Vigo, T. L., Kinzig, J., Eds.; VCH Publishers: New York, 1992; pp 67–106.

(6) Wierschke, S. G. *Mater. Res. Soc. Symp. Proc.* **1989**, *134*, 313–327.

(7) Allen, S. R.; Fillipov, A. G.; Farris, R. J.; Thomas, E. L.; Wong, C.-P.; Berry, G. C.; Cheveney, E. C. *Macromolecules* **1981**, *14*, 1135–1138.

(8) DePra, P. A.; Gaudiello, J. G.; Mark, T. J. *Macromolecules* **1988**, *21*, 2295–2297.

(9) (a) Vanherzeele, H.; Meth, J. S.; Jenekhe, S. A.; Roberts, M. F. *Appl. Phys. Lett.* **1991**, *58*, 663–665. (b) Vanherzeele, H.; Meth, J. S.; Jenekhe, S. A.; Roberts, M. F. *J. Opt. Soc. Am. B* **1992**, *9*, 524–533.

(10) Roberts, M. F.; Jenekhe, S. A.; Cameron, A.; McMillan, M.; Perlstein, J. *Chem. Mater.*, in press.

(11) Welsh, W. J.; Bhaumik, D.; Mark, J. E. *Macromolecules* **1981**, *14*, 947–950.

(12) Wellman, M. W.; Adams, W. W.; Wolff, R. A.; Dudis, D. S.; Wiff, D. R.; Fratini, A. V. *Macromolecules* **1981**, *14*, 935–939.

(13) Bhaumik, D.; Welsh, W. J.; Jaffe, H. H.; Mark, J. E. *Macromolecules* **1981**, *14*, 951–953.

0897-4756/93/2805-1744$04.00/0

acid (MSA) and chlorosulfonic acid (CSA). As a result, processing of PBZT into useful forms such as thin films, coatings, or fibers has been extremely difficult.

It was recently reported from our laboratory[14,15] that PBZT and many other rigid-chain polymers can be solubilized in aprotic organic solvents such as nitroalkanes and nitrobenzene, in the presence of a metal halide Lewis acid (e.g., $AlCl_3$, $GaCl_3$, $FeCl_3$, etc.). PBZT solutions in organic solvents were thus prepared with sufficiently high concentrations that liquid crystallinity was observed.[14,16] The critical concentration for observing liquid crystallinity was found to depend on the type and concentration of Lewis acid used.[16] We proposed[14,15] that the Lewis acids form coordination complexes with the heteroatom (N,S) ligands of PBZT and that these complexes are the soluble species. Stoichiometries of 4 mol of Lewis acid/mol of PBZT repeat unit necessary for complete solubilization supported this picture, as did the absence of any evidence of π-electron charge-transfer complexation. Reversibility of the complexation by coagulation in a strong Lewis base suggested that our approach holds promise for the large-scale processing of PBZT and other heterochain polymers.[14-16] For example, we were able to use this soluble coordination complex approach to prepare good optical quality thin films of PBZT and PBZT molecular composites[17] and studied their nonlinear optical properties in some detail.[9]

It is our purpose in this paper to examine the details of our proposed mechanism of complexation and solubilization of PBZT in organic solvents. The preparation of complexes of PBZT with the Lewis acids BCl_3, $AlCl_3$, and $GaCl_3$ in various solvents and their solubilization in suitable organic solvents are reported. We present studies of the structures of these complexes with emphasis on elucidation of the sites of Lewis acid coordination and discuss the solution and solid state properties of the complexes. In studies to be reported in a subsequent paper[10] we use a computational modeling approach to gain an understanding of the effects of Lewis acid coordination complexation on the structure and properties of PBZT.

Experimental Section

Materials. PBZT was synthesized according to literature methods.[1,2] The intrinsic viscosity of the PBZT sample measured in MSA at 30 °C was 17.8 dL/g. The estimated weight-average molecular weight was 29 023 for the sample by using the known Mark–Houwink relationship for this polymer:[2] $[\eta] = 1.65 \times 10^{-7} M_w^{1.8}$. A model compound for PBZT, 2,6-diphenylbenzo[1,2-*d*:4,5-*d*′ bisthiazole] (t-DBZT) was provided to us by the Air Force Materials Laboratory, Dayton, OH. The sample was recrystallized twice from toluene and thoroughly dried in a vacuum oven prior to use. The organic solvents, Lewis acids, and protic acids were used as received, without further purification: nitromethane, 99+% (Aldrich); dichloromethane, 99+% (Aldrich); aluminum(III) chloride ($AlCl_3$), 99.99% (Aldrich); gallium(III) chloride ($GaCl_3$) 99.9999% (Alfa); boron(III) chloride (BCl_3) as a 1.0 M solution in dichloromethane (Aldrich); methanesulfonic acid, 99% (Aldrich).

Preparation of Complexes. Due to the moisture sensitivity of the group III metal halides used, all polymer complexes were prepared in a Vacuum Atmospheres Dri-Lab filled with nitrogen. A Dri-Train assembly attached to the glovebox circulated the gas to remove residual oxygen and water vapor to a level of 1–5 ppm. Although some of the complexes could be prepared in the ambient laboratory environment which is much higher in oxygen or moisture content than the glovebox, excess Lewis acid above the stoichiometric requirements was needed to do so. Solutions of such complexes prepared in ambient air gave large polymer precipitates over time and the solid complexes gradually reverted to the pure PBZT containing the hydrated metal halides. For accurate studies therefore, it was necessary to prepare complexes in the inert atmosphere of the glovebox.

Nitromethane (NM) was found to be the most suitable solvent for preparation of solutions of PBZT complexes. Solutions of the complexes of PBZT with $AlCl_3$ and $GaCl_3$ were prepared as follows. A specific amount of Lewis acid was weighed and added to nitromethane. The mixture was stirred at room temperature until the Lewis acid was completely dissolved. A known weight of PBZT was then added to the solution and the mixture was stirred until the polymer was completely dissolved. Dissolution of PBZT commences immediately when it is added to the nitromethane/Lewis acid at room temperature as indicated by the change of solution color from colorless to yellow within a few seconds of adding the polymer. The preparation of concentrated solutions took several days for complete dissolution of the polymer but could be accelerated by heating at 40–60 °C. The amount of Lewis acid Y (grams) necessary for complete polymer dissolution was calculated using the formula

$$rX/266.3 = Y/M_r \quad (1)$$

X is the amount of PBZT used (grams); 266.3 is the molecular weight of the polymer repeat unit taken as $C_{14}H_6N_2S_2$; M_r is the molecular weight of the Lewis acid and r is the minimum number of moles of Lewis acid required per mole of polymer repeat unit. We found r for $AlCl_3$ complexes to be 4.0×0.05 and for $GaCl_3$ complexes r is 4.5 ± 0.20. Solutions of PBZT complexes thus prepared were stable over a period of many months without apparent loss in viscosity or visible polymer precipitation when stored in a glovebox. Solid PBZT/Lewis acid complexes were prepared from these solutions by slow evaporation of NM in vacuum at 60–70 °C for 10–12 h.

PBZT complexes with BCl_3, $AlCl_3$, and $GaCl_3$ were also prepared in dichloromethane (DCM). In this case the complexes do not dissolve and complexation proceeds by heterogeneous reaction of the dissolved Lewis acid with the solid polymer. The procedure was as follows. A solution of the Lewis acid in DCM of known concentration was prepared. Thin films of PBZT were added to the solution which was then stirred for 5–7 days. Complexes of various stoichiometries (r = 1–10) were prepared in this way by using the appropriate amount of Lewis acid for a given polymer sample, determined by using eq 1. 1.0 M solutions of BCl_3 in DCM were used. The solubility of $AlCl_3$ in DCM is limited to about 1 wt %. $GaCl_3$ dissolves readily in DCM and solutions of 20 wt % $GaCl_3$ or higher were readily prepared. The solid complexes formed were removed from solution and dried in vacuum as described above, except for the gallium trichloride complexes used for differential scanning calorimetry and the boron trichloride complexes which were dried at room temperature in the drybox.

Complexes of PBZT for infrared spectroscopy were (a) thin films cast on NaCl substrates from NM solutions or (b) freestanding films prepared in DCM. We prepared complexes of PBZT with stoichiometries (ratio of Lewis acid to PBZT repeat unit) intermediate between 0:1 and 4:1 for the infrared studies. Solid samples for UV–visible–NIR spectroscopy were ~0.1-μm thin films sandwiched between 1-mm-thick optically flat silica substrates. Solutions for UV–visible–NIR and fluorescence spectroscopies were $\sim 10^{-4}$ and 10^{-5} M in PBZT repeat unit, respectively, contained in quartz cells. Solutions of PBZT complexes for NMR spectroscopy contained 1–3 wt % polymer in deuterated NM. Samples of PBZT complexes for dynamic mechanical analysis (DMA) were thin films (~1 μm) sandwiched between glass microscope slides (55 × 20 × 1 mm). The DMA samples were cast films pressed (10 kg weight) between the glass slides.

(14) (a) Jenekhe, S. A.; Johnson, P. O.; Agrawal, A. K. *Macromolecules* **1989**, *22*, 3216–3222. (b) Jenekhe, S. A.; Johnson, P. O. *Macromolecules* **1990**, *23*, 4419–4429.

(15) Roberts, M. F.; Jenekhe, S. A. *Polym. Prepr. (Am. Chem. Soc., Div. Polym. Chem.)* **1990**, *31* (2), 480–481.

(16) Roberts, M. F.; Jenekhe, S. A. *Polym. Commun.* **1990**, *31*, 215–217.

(17) Roberts, M. F.; Jenekhe, S. A. *Chem. Mater.* **1990**, *2*, 629–631.

Instruments and Methods. Fourier transform infrared (FTIR) spectroscopy was done by using a Nicolet 20SXC FTIR spectrometer at a resolution of 4 cm^{-1}. Sets of 32 scans were signal averaged, and the resulting spectra were stored on a disk. Internal calibration of the frequency scale was done to an accuracy of 0.2 cm^{-1} by using a He–Ne laser. All spectra were taken at room temperature (25–27 °C) under nitrogen purge. UV–visible–NIR (UV–vis) spectra were collected on a Perkin-Elmer Lambda 9 spectrophotometer. Fluorescence spectra were taken on a Spex Fluorolog-2 spectrofluorimeter which was controlled by a Spex DM 3000f computer. NMR spectra were obtained using a General Electric Model QE400 spectrometer. For ^{71}Ga NMR experiments, a 0.5 M aqueous solution of $GaCl_3$ was used to obtain a reference and a similar solution of $AlCl_3$ was used as a reference in ^{27}Al NMR experiments. The sharp resonances of $Ga(H_2O)_6^{3+}$ and $Al(H_2O)_6^{3+}$ were taken as the 0 ppm reference in the chemical shift scale in ^{71}Ga and ^{27}Al NMR experiments, respectively. Thermal analysis was done with a du Pont Model 2100 TA system which is based on an IBM PS/2 computer. Thermogravimetric analysis (TGA) scans were carried out at a heating rate of 10 °C/min under a nitrogen purge. TGA runs were started after allowing the samples to equilibrate at 25–30 °C in nitrogen for a period of 15–20 min. Weight loss during this equilibration time was less than 1%. Differential scanning calorimetry (DSC) was also done under a nitrogen purge at a heating rate of 20 °C/min. Indium (mp 156.6 °C) standard was used to calibrate the DSC instrument. Elemental analysis was done by Galbraith Laboratories, Inc. (Knoxville, TN). DMA experiments were done on a Rheometrics Model RSAII solids analyzer by using liquid nitrogen as a coolant. A three-point unclamped bending test was used. Measurements were taken every 3 °C with a thermal soak time of 1 min.

Results and Discussion

Preparation of Complexes. The simultaneous complexation and dissolution of PBZT in Lewis acid/nitromethane and other nitroalkanes or nitrobenzene is feasible because of the combination of poor electron-donating and good polar properties of these organic solvents. Nitromethane (NM) has a very low tendency toward electron donation, as measured by its donor number (DN) of 2.7,[18] its enthalpy of interaction with BF_3 (ΔH_{BF_3}) of −37.6 kJ/mol,[19] its donor strength (D_S) of 9,[20] the wavelength of the complex it forms with Cu(tmen)(acac)$^+$ (Cu(λ_{max})) which is 532 nm[21] and its Drago parameters.[22] This low electron-donating ability or weak Lewis basicity means that competition between NM and the polymer ligands (N and S heteroatoms of PBZT) for the Lewis acid will be minimal. The high polarity of NM as measured by its dielectric constant ϵ (35.9) and dipole moment μ (3.46 D)[23] allows it to easily solubilize many Lewis acids and the polar complexes they form with PBZT.

On the other hand dichloromethane (DCM) is an ideal medium for polymer complex formation without dissolution. DCM also has a low electron-donating ability (DN ≈ 0, $\Delta H_{BF_3} = -10$ kJ/mol, $D_S = 7$, Cu(λ_{max}) = 550 nm) and so allows efficient complex formation, and its low polarity ($\epsilon = 8.9$ and $\mu = 1.60$ D) effectively prevents the complexes formed from dissolving.

The complexes PBZT forms with Lewis acids in DCM are the same as those prepared in NM. PBZT/$AlCl_3$ and PBZT/$GaCl_3$ complexes prepared in DCM with sufficient

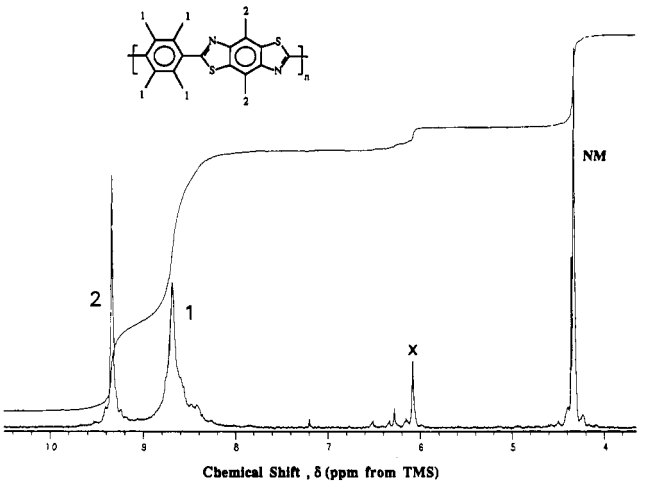

Figure 1. ^1H NMR spectrum of PBZT in $GaCl_3$/deuterated nitromethane.

Lewis acid can be dissolved in NM. BCl_3 is a gas at room temperature and as such presents difficulties in quantitative studies of its complexes. However complexes of PBZT formed in BCl_3/DCM can be at least partially dissolved in NM. Prolonged exposure (about 1 h) of the solid PBZT/BCl_3 complexes to nitrogen (in the drybox) or air results in their complete decomplexation to the pure PBZT and the sublimation of the Lewis acid.

Structures of PBZT Complexes: Solution Studies. Figure 1 shows the typical ^1H NMR spectrum of PBZT in Lewis acid/deuterated nitromethane solution. The minor impurity peak at about 6.1 ppm in Figure 1 is due to the solvent ($GaCl_3$/NM) and the peak labeled "NM" at 4.33 ppm is due to nitromethane. The aromatic proton resonances are at 8.7 and 9.35 ppm in $GaCl_3$/NM. The 8.7 ppm resonance is due to the four protons on the phenylene ring of the repeat unit and the 9.35 ppm resonance is due to the two protons of the benzobisthiazole ring. Integration gives the expected 2:1 ratio for the 8.7 ppm:9.35 ppm peak areas. In $AlCl_3$/NM the same spectrum was obtained for the aromatic protons of PBZT, namely, the polymer resonances were again at 8.7 and 9.35 ppm. The fact that each type of proton resonates at the same frequency in $AlCl_3$/NM and $GaCl_3$/NM shows that the effect of electron withdrawal from PBZT by the Lewis acid on the resonance frequency is the same for both $AlCl_3$ and $GaCl_3$. Assignment of the 9.35 ppm resonance to the protons on the benzobisthiazole ring is consistent with previous assignments for derivatives of PBZT which contained the basic benzobisthiazole unit in the repeat unit.[24] In this previous study the ^1H NMR spectra of three polymers were reported: poly(benzobisthiazole) (PBBT), poly(benzobisthiazole-2,6-diylvinylene) (PBTV), and poly(benzobisthiazole-2,6-diyldivinylene) (PBTDV), wherein the phenylene segment of the PBZT repeat units is respectively absent, replaced by vinylene and divinylene linkages. The benzobisthiazole proton resonances in PBBT, PBTV, and PBTDV were observed at 8.9–9.2, 9.2–9.33, and 9.02 ppm, respectively. Thus the effect of such structural changes to PBZT does not significantly affect the position of the resonances of the benzobisthiazole protons since all are close to 9.35 ppm, despite the fact that these structural changes have considerable influence on the electronic

(18) Gutmann, V. *The Donor-Acceptor Approach to Molecular Interactions*; Plenum Press: New York, 1978; p 20.
(19) Maria, P. C.; Gal, J. F. *J. Phys. Chem.* **1985**, *89*, 1296–1304.
(20) Persson, I. *Pure Appl. Chem.* **1986**, *58*, 1153–1161.
(21) Soukup, R. W.; Schmid, R. *J. Chem. Educ.* **1985**, *62*, 459–462.
(22) Drago, R. S. *Struct. Bonding (Berlin)* **1973**, *15*, 73.
(23) Reichardt, C. *Solvents and Solvent Effects in Organic Chemistry*, 2nd ed.; VCH Publishers: New York, 1988; pp 408–409.
(24) Osaheni, J. A.; Jenekhe, S. A. *Chem. Mater.* **1992**, *4*, 1282–1290.

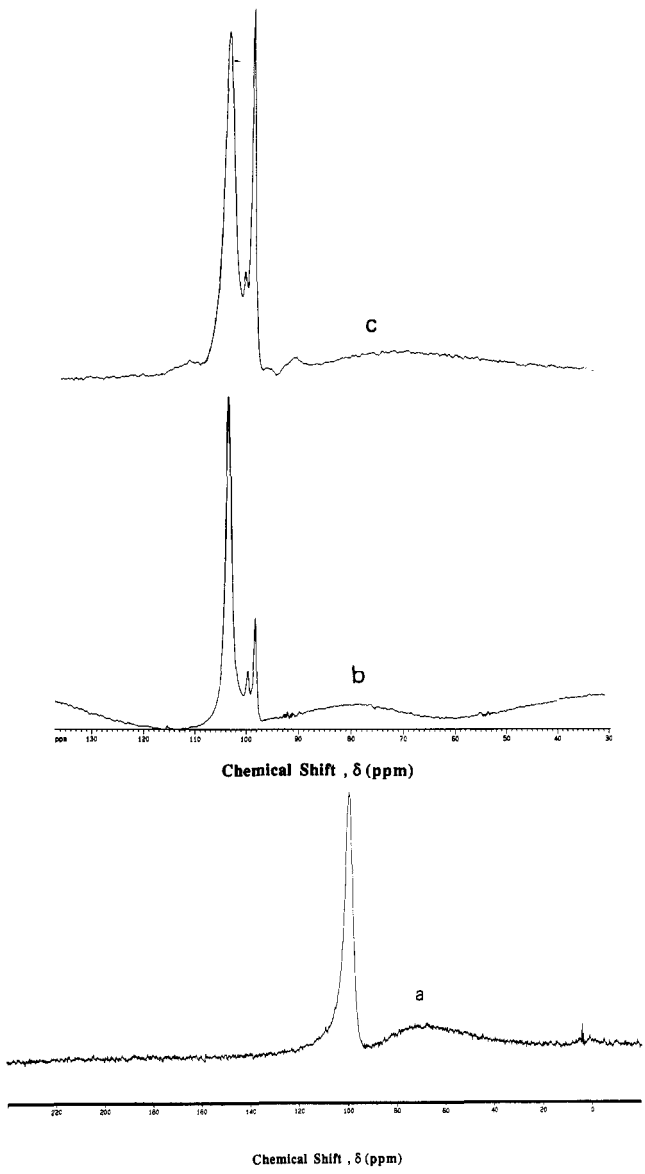

Figure 2. ^{27}Al NMR spectra of (a) $AlCl_3$, (b) 4.20:1 $AlCl_3$:PBZT, and (c) 5.29:1 $AlCl_3$:PBZT, in deuterated nitromethane. Ratios are mole ratios of $AlCl_3$ to polymer repeat unit in solution.

structure of PBZT, namely they lower the π–π^* transition energy by up to 0.4eV.

The ^{27}Al NMR spectra of $AlCl_3$/NM, $AlCl_3$:PBZT (4.20:1)/NM, and $AlCl_3$:PBZT (5.29:1)/NM solutions are shown in Figure 2a–c, respectively. In Figure 2a, the Al resonance is at 98 ppm and is due to $AlCl_3$ solvated by nitromethane. In Figure 2b the spectrum shows sharp resonances at 98 ppm and 103 ppm which indicate that there are two main Al species present in solution. The species which gives rise to the 98 ppm peak is $AlCl_3$ solvated by nitromethane as in Figure 2a, which we refer to as "free" $AlCl_3$. The species giving rise to the 103 ppm peak is $AlCl_3$ coordinated to the PBZT, which we refer to as "coordinated" $AlCl_3$. Thus electron donation from PBZT causes a downfield shift of the Al resonance by 5 ppm relative to "free" $AlCl_3$. These resonances are in the expected region for tetrahedrally coordinated aluminum (40–140 ppm).[25] Integration of the spectrum in Figure 2b gave a ratio of 0.46:4 for

(25) Akitt, J. W. In *Multinuclear NMR*; Mason, J. Ed.; Plenum Press: New York, 1987; pp 447–461.

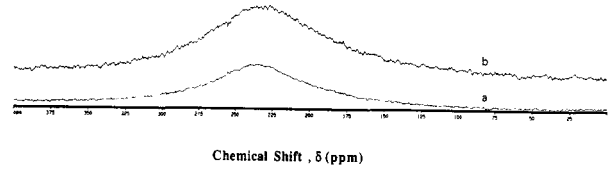

Figure 3. ^{71}Ga NMR spectra of (a) $GaCl_3$ and (b) 5.0:1 $GaCl_3$:PBZT repeat unit, in deuterated nitromethane.

"free" to "coordinated" aluminum. This ratio is approximate due to peak overlap and the minor peak at 99 ppm. We estimated the possible error to be ±5%. The solution of Figure 2b was prepared with a ratio 4.20:1 of $AlCl_3$:PBZT repeat unit. Thus for a complex in which 4 mol of Lewis acid are coordinated to each repeat unit in the polymer, the ratio of "free":"coordinated" aluminum in this solution would be 0.20:4. This is close to the ratio obtained from integration. The small differences between these ratios (0.20:4 and 0.46:4) may arise from two possible sources: (1) the approximation made in the spectral integration or (2) there may be uncomplexed sites (N or S atoms) in the polymer. If the latter is the case, then less than 6% of available sites may be uncomplexed, i.e., approximately one in every sixteen N or S atoms may be uncomplexed. The spectrum of the $AlCl_3$:PBZT solution in Figure 2c again shows the two resonances at 98 ppm and 103 ppm representing "free" and "coordinated" aluminum, respectively. Integration gives a value of 1.80:4 for "free":"coordinated" aluminum. The solution used to obtain this spectrum was prepared with a ratio 5.29:1 of $AlCl_3$:PBZT repeat unit. From this we expect a ratio of 1.29:4 of "free":"coordinated" aluminum in solution for a complex in which there are 4 mol of Lewis acid coordinated to each mole of polymer repeat unit. Comparing the above ratios of 1.80:4 and 1.29:4, if the difference does not arise from the approximation made in the spectral integration, then about 9% of the coordination sites (about one in every eleven heteroatoms) may be uncomplexed. Our earlier observation was that a ratio of 4:1 $AlCl_3$:PBZT repeat unit is necessary for polymer solubilization. The results in Figure 2 show that with this stoichiometry, practically all of the Lewis acid is coordinated to PBZT, and any excess will simply remain solvated in nitromethane. In the next section we show that the coordination sites are indeed the nitrogen and sulfur heteroatoms.

The ^{71}Ga NMR spectra of $GaCl_3$/NM and $GaCl_3$:PBZT (5.0:1)/NM solutions are shown in Figure 3. The spectra in Figure 3 show resonances which are much broader and shifted downfield (centered at ~230 ppm) compared to the $Ga(H_2O)_6^{3+}$ ion used as reference (0 ppm), as expected for gallium species of lower coordination number.[25] The broadness of the resonances makes it difficult to distinguish the differences between the two spectra of Figure 3.

Figure 4 shows the optical absorption spectra of PBZT solutions in $AlCl_3$/NM and methanesulfonic acid (MSA). The corresponding absorption maxima are 441 and 443 nm in the two solvents, respectively. The optical absorption spectrum of a PBZT solution in $GaCl_3$/NM (not shown) is similar to that in $AlCl_3$/NM shown in Figure 4. The absorption maximum in $GaCl_3$/NM is 441 nm. The maximum molar absorptivities of the PBZT complexes are 6.3×10^4, 5×10^4, and 4.4×10^4 L mol^{-1} cm^{-1} and the band edges are at 467, 470, and 469 nm in $AlCl_3$/NM, $GaCl_3$/NM, and MSA respectively. The spectra are similar in all three solvents although the PBZT/Lewis acid complexes have higher absorption coefficients than PBZT in MSA.

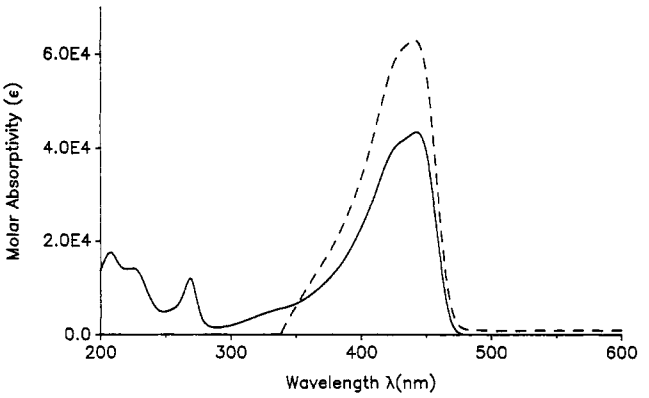

Figure 4. UV–visible spectrum of 10^{-4} M PBZT in $AlCl_3$/NM (dashed line) and in MSA (solid line). Units of ϵ are L mol^{-1} cm^{-1}.

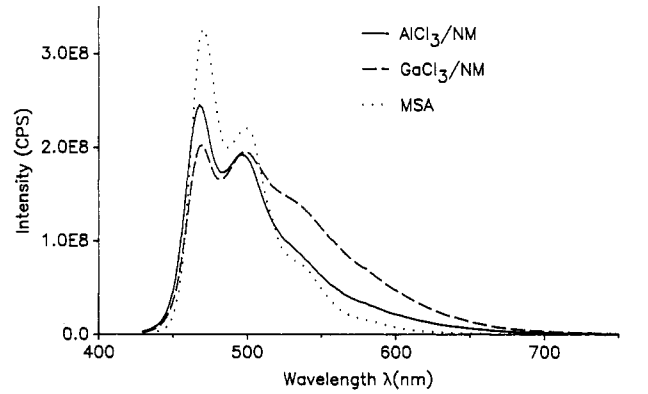

Figure 5. Fluorescence spectra of (10^{-5} M) PBZT in $AlCl_3$/NM (solid line), $GaCl_3$/NM (dashed line), and MSA (dotted line) with an excitation wavelength of 420 nm.

Figure 5 shows the fluorescence spectra of PBZT solutions in $AlCl_3$/NM, $GaCl_3$/NM, and MSA with an excitation wavelength of 420 nm. The main emission peak in all three solutions is at 467 nm, and there is a minor peak at 494 nm. The PBZT emission spectrum in MSA solution is similar to that reported earlier by others.[26] The spectrum obtained in MSA is narrower than in either $AlCl_3$/NM or $GaCl_3$/NM. The shoulder band at about 540 nm in $GaCl_3$/NM is much more pronounced than in MSA. The spectrum for the $AlCl_3$/NM solution is intermediate between the two in this respect. The high wavelength spectral tail is significant to much higher wavelength in $GaCl_3$/NM and $AlCl_3$/NM than in MSA. These differences may point to different excited state relaxation mechanisms of PBZT/Lewis acid complexes in nitromethane compared to protonated PBZT in MSA solution.

The optical absorption spectra of the t-DBZT model compound in various solvents are shown in Figure 6. The

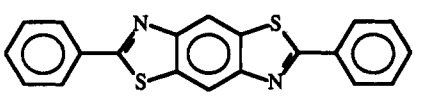

t-DBZT

$AlCl_3$ and $GaCl_3$ complexes of t-DBZT in nitromethane exhibit similar spectra. The molar absorptivities are approximately 5×10^4 L mol^{-1} cm^{-1}, the absorption maxima

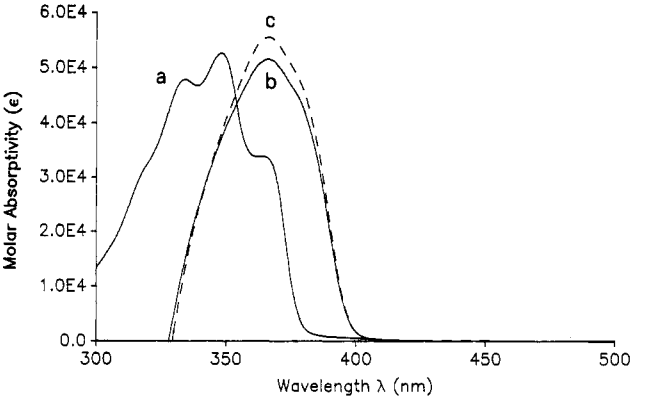

Figure 6. UV–visible spectra of t-DBZT dissolved ($\sim 10^{-4}$ M in) (a) dichloromethane, (b) $AlCl_3$/NM, and (c) $GaCl_3$/NM. Units of ϵ are L mol^{-1} cm^{-1}.

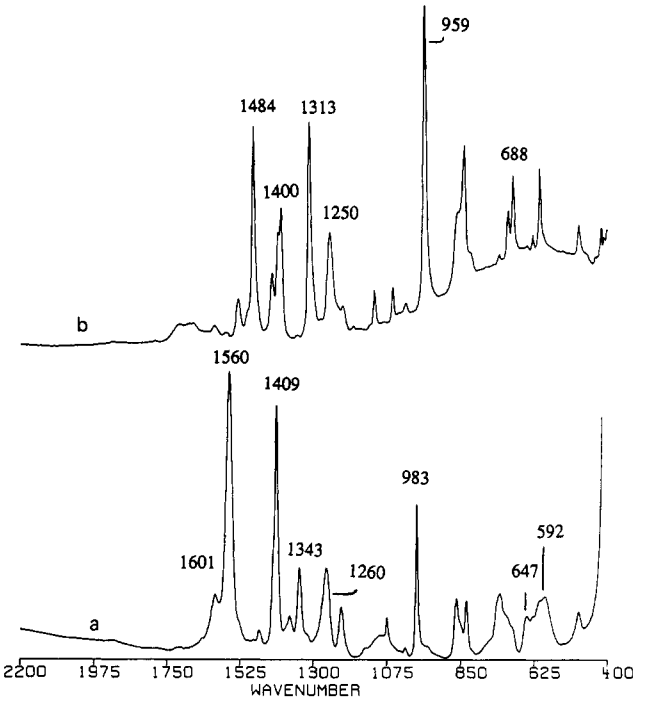

Figure 7. FTIR spectra of (a) 1:4 PBZT:$GaCl_3$ complex, (b) PBZT. Ratio in (a) is mole ratio of PBZT repeat unit to $GaCl_3$.

are 365 nm and the band edges are 396 nm in both solvents. Interestingly the spectrum of t-DBZT in dichloromethane (Figure 6a) is blue-shifted relative to the absorption spectra of its complexes (Figure 6b,c). The band edge is at 378 nm, and there is vibrational structure evident in the main absorption band with a maximum at 347 nm. The significant red-shift of the electronic spectra of the t-DBZT complexes relative to the pure compound suggest that electronic delocalization is increased in the complexes. Theoretical evidence supporting this view is presented in a following paper.[10]

Structures of PBZT Complexes: Solid-State Studies. Figure 7 shows the FTIR spectra of PBZT (b) and the 1:4 PBZT:$GaCl_3$ complex (a). Figure 8 shows the spectra of the 1:1 (a), 1:2 (b), and 1:3 (c) PBZT:$GaCl_3$ complexes. The 1484-cm^{-1} band of PBZT in Figure 7b is primarily the C=N stretching vibration.[27] This band gradually diminishes from the 1:0 case (Figure 7b) until it completely disappears in the 1:4 complex (Figure 7a).

(26) Wang, F. W.; Lowry, R. E.; Fanconi, B. M.; Heilweil, E. J. *Polym. Mater. Sci. Eng.* **1987**, *57*, 336–340.

(27) Shen, D. Y.; Hsu, S. L. *Polymer* **1982**, *23*, 969–973.

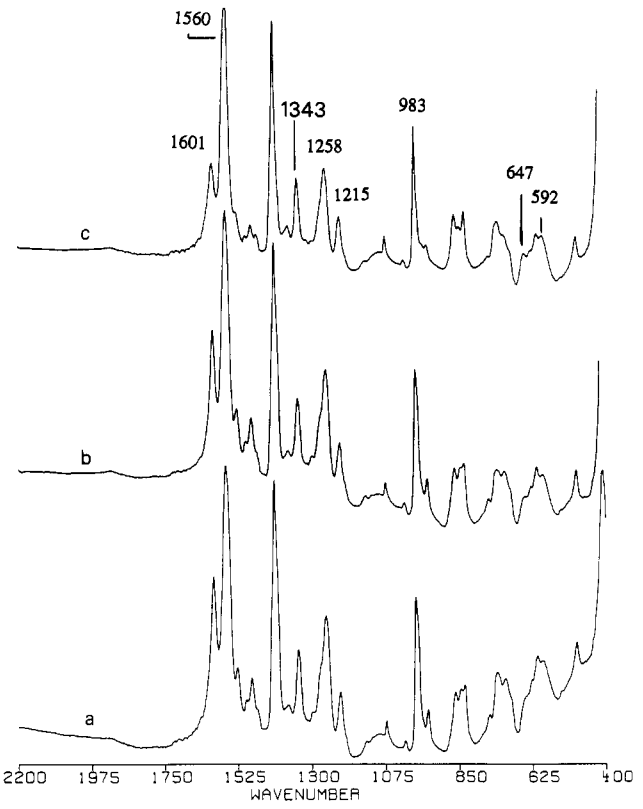

Figure 8. FTIR spectra of PBZT:$GaCl_3$ complexes: (a) 1:1, (b) 1:2, (c) 1:3; ratios as in Figure 7.

A quantitative comparison with the pure PBZT films showed that in the 1:1 complex of Figure 8a the 1484-cm^{-1} band has ~48% of its original intensity, 39% in the 1:2 complex (Figure 8b), and 17% in the 1:3 complex (Figure 8c). In place of the 1484-cm^{-1} band is an intense band at 1560 cm^{-1} which we assign to the C=N stretch of $GaCl_3$ coordinated nitrogens in PBZT. Similar shifts have been reported for C=N stretch modes of Lewis acid coordinated polyazomethines[28] and other Schiff's bases.[29a] The shift of this band to higher frequency has been rationalized on the basis of a rehybridization model[29b] wherein results of ab initio calculations were used to show that coordination to imine nitrogens leads to an increase in the C=N stretching force constant.

IR absorption bands at 1400 and 1313 cm^{-1} in PBZT (Figure 7b) have been assigned to the heterocyclic ring stretches,[27] mostly associated with C–N vibrations. These bands are also strongly affected by $GaCl_3$ coordination to nitrogen. The 1400-cm^{-1} band shifts to 1372 cm^{-1} and becomes weaker because of decreased overlap with the 1409-cm^{-1} phenylene ring in-plane vibration. The 1313-cm^{-1} band becomes less intense and shifts to 1343 cm^{-1} in the 1:4 complex (Figure 7a).

The band at 688 cm^{-1} in PBZT has also been assigned to a heterocyclic ring stretch.[27] On the basis of similar values reported for sulfur-containing small-molecule compounds,[30,31] we assign it to C–S stretching. This band is of medium intensity in PBZT. In the 1:1 complex of Figure 8a it has lost intensity relative to PBZT and is replaced by a band of gradually increasing intensity from the 1:1 to 1:4 stoichiometries, at 647 cm^{-1}. We attribute this effect to coordination of the sulfur atoms, the 647- and 688-cm^{-1} bands indicating complexed and uncomplexed S species respectively.

Several other prominent bands in the PBZT spectrum not specifically associated with vibrations about the heteroatoms are significantly affected by complexation. A band, not clearly visible in PBZT, appears at 1601 cm^{-1} in the 1:1 complex in Figure 8a and gradually loses intensity until it is only a weak band in the 1:4 spectrum in Figure 7a. A band at this frequency has been assigned to the symmetric phenylene ring stretch in the Raman spectrum of PBZT.[32] The Raman intensity of this band was related to $\cos^2\theta$, the out-of-plane twist angle of the phenylene ring. It is most likely a combination of symmetry considerations and ring twist which lead to the appearance of this band in the FTIR spectra of the complexes. The 1:4 complex, a species of similar symmetry to PBZT with all four heteroatoms coordinated by $GaCl_3$, exhibits the lowest intensity of the 1601-cm^{-1} band (Figure 7a). The absorption at 1250 cm^{-1} was assigned as the "crystalline" band of PBZT, and it was proposed that this band is sensitive to intermolecular interactions.[27] It is shifted on complexation with $GaCl_3$, appearing at 1256 cm^{-1} in 1:1 and 1:2 complexes, 1258 cm^{-1} in the 1:3 complex, and 1260 cm^{-1} in the 1:4 complex. The adjacent band at 1210 cm^{-1} in PBZT which is the C–C stretch of the carbons joining the phenylene and benzobisthiazole rings, shifts to ~1214 cm^{-1} in 1:1 and 1:2 complexes and then to 1215 cm^{-1} in 1:3 and 1:4 complexes, indicating a gradual increase in bond order. The very prominent 959-cm^{-1} "breathing" mode of the benzobisthiazole rings is gradually eliminated and replaced by a 983-cm^{-1} band on complexation.

There is a new band present in the spectra of all four complexes at 592 cm^{-1}. Its intensity is greatest in the 1:4 complex in Figure 7a. There is no band at this frequency in PBZT. We tentatively assign it to the stretching vibration of the gallium-heteroatom (N or S) coordinate covalent bonds. Similar bands, appearing further into the far-IR region, have been reported for this type of bond in transition-metal complexes,[33] and it is on this basis that we make the assignment.

The FTIR spectra of the PBZT/$AlCl_3$ and PBZT/BCl_3 complexes are shown in Figure 9a,b respectively. For the PBZT/$AlCl_3$ complex (Figure 9a) a large excess of $AlCl_3$ over the minimum necessary for solubilization in nitromethane was used to prepare the complex in dichloromethane. In this complex the C=N stretch is at 1556 cm^{-1}, the C–N vibrations are at 1370 and 1342 cm^{-1} and the 688-cm^{-1} band splits into two at 681 and 651 cm^{-1}. Other bands discussed above for the PBZT/$GaCl_3$ complexes are observed here at 1263, 1212, 983, and 559 cm^{-1}. The elimination of the 1484 cm^{-1} band and shifts of the C–N bands are again evidence of coordination to the nitrogens of PBZT. The band at 681 cm^{-1} indicates that

(28) (a) Yang, C. J.; Jenekhe, S. A. *Mater. Res. Soc. Symp. Proc.* **1992**, *277*, 197–204. (b) Yang, C. J.; Jenekhe, S. A.; Meth, J. S.; Vanherzeele, H. *Polym. Adv. Technol.*, in press.

(29) (a) Lopez-Garriga, J. J.; Babcock, G. T.; Harrison, J. F. *J. Am. Chem. Soc.* **1986**, *108*, 7241–7251. (b) Lopez-Garriga, J. J.; Hanton, S.; Babcock, G. T.; Harrison, J. F. *J. Am. Chem. Soc.* **1986**, *108*, 7251–7254.

(30) Lin-Vien, D.; Colthup, N. B.; Fateley, W. G.; Grasselli, J. G. *The Handbook of Infrared and Raman Characteristic Frequencies of Organic Molecules*; Academic Press: New York, 1991; pp 225–232.

(31) Frolov, Y. L. In *Chemistry of Organosulfur Compounds*; Belen'kii, L. I. Ed.; Ellis Horwood: New York, 1990; pp 255–265.

(32) Shen, D. Y.; Venkatesh, G. M.; Burchell, D. J.; Shu, P. H. C.; Hsu, S. L. *J. Polym. Sci., Polym. Phys. Ed.* **1982**, *20*, 509–521.

(33) (a) Weaver, J. A.; Hambright, P.; Talbert, P. T.; Kang, E.; Thorpe, A. N. *Inorg. Chem.* **1970**, *9*, 268–273. (b) Duff, E. J.; Hughes, M. N.; Rutt, K. J. *J. Chem. Soc. A* **1968**, 2354–2357, (c) Chan, N. N. Y.; Goodgame, M.; Weeks, M. J. *J. Chem. Soc. A* **1968**, 2499–2501.

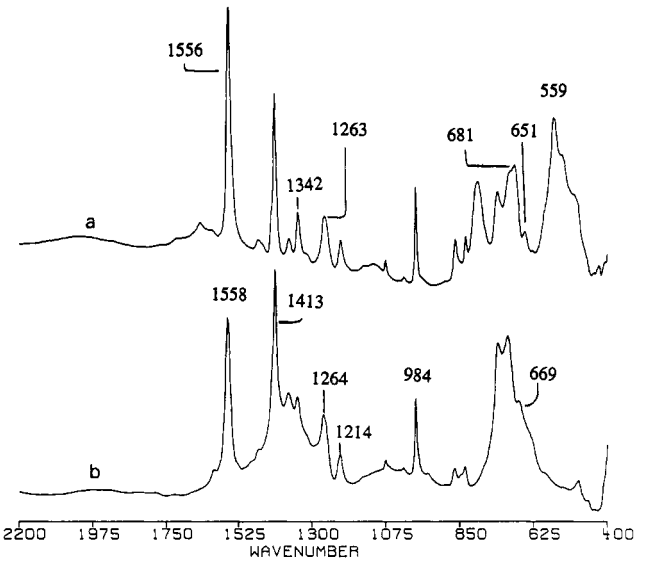

Figure 9. FTIR spectra of (a) PBZT/$AlCl_3$ complex prepared in dichloromethane with 10 mol of $AlCl_3$/mol PBZT repeat unit, (b) PBZT/BCl_3 complex prepared in dichloromethane with the same ratio as in (a).

although there is coordination to sulfur (the 651 cm^{-1} band), there are some uncomplexed sulfur atoms. The 1:4 PBZT:$AlCl_3$ complex cast from nitromethane had the same spectrum as Figure 9a except that absorptions below ~700 cm^{-1} were buried under the intense absorption of the NaCl substrate in that region. The PBZT/BCl_3 complex of Figure 9b shows bands at 1558, 1371, 1345, 1264, 1214, and 984 cm^{-1} and a shoulder band at 669 cm^{-1}. This complex was also prepared using a large excess of BCl_3 over 1:4 in dichloromethane.

Finally with regard to the infrared spectra of all the PBZT complexes of Figures 7–9, we found that exposure of each to air for short periods (<5 min) resulted in very different spectra. The bands of pure PBZT were observed as in Figure 7b accompanied by very broad absorptions at 3600–3000, 1750–1550, and 750–400 cm^{-1} due to stretching and scissoring vibrations of absorbed water molecules and hydrated metal halide vibrations. The complexes are thus sensitive to moisture, and exposure to ambient moisture in air leads to rapid decomplexation of PBZT and hydration of the Lewis acids.

Elemental analysis of pure PBZT[14a] gave C 61.84%, N 10.06%, S 23.2%, H 2.34% corresponding to $C_{14}H_{6.36}N_{1.95}S_{1.97}$ compared to an expected C 63.11%, N 10.52%, S 24.14%, H 2.25% based on a repeat unit of $C_{14}H_6N_2S_2$ and neglecting end groups and defects. Despite the moisture sensitivity of PBZT complexes, we also submitted a sample of the PBZT/$GaCl_3$ complex for elemental analysis. Since the complex prepared in NM requires an excess over 1:4 stoichiometry for solubilization, the complex was washed with DCM to dissolve any excess (uncomplexed) Lewis acid. The results obtained were C 17.62%, N 3.58%, S 6.93%, H 1.56%, Ga 23.28%, Cl 40.19% corresponding to $C_{14}H_{14.87}N_{2.44}S_{2.06}Ga_{3.20}Cl_{10.79}$. With 1:4 stoichiometry and the repeating unit structure given above, we expect C 17.30%, N 2.88%, S 6.61%, H 0.62%, Ga 28.71%, Cl 43.87% ($C_{14}H_6N_2S_2Ga_4Cl_{12}$). The absolute carbon content is close to that expected, and the nitrogen and sulfur values are reasonable. However there is a large error in hydrogen and an apparent shortfall in gallium and chlorine. These may be due to experimental

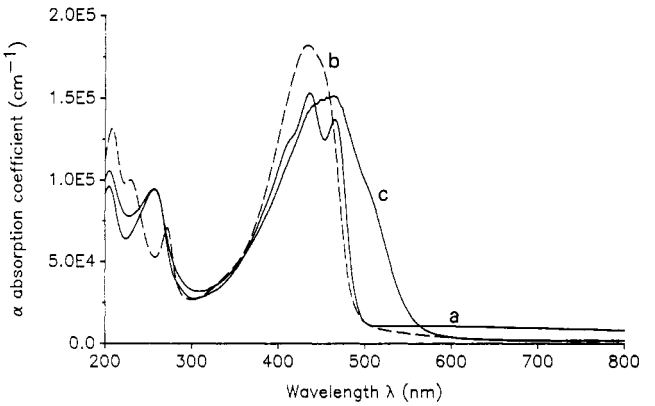

Figure 10. UV-visible absorption spectra of thin films of (a) PBZT (solid line), (b) PBZT/$AlCl_3$ complex (dashed line), (c) PBZT/$AlCl_3$ complex after exposure to air for 3 min (solid line).

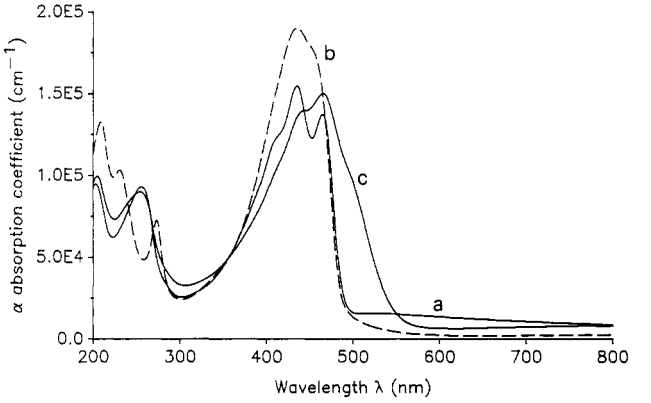

Figure 11. UV-visible absorption spectra of thin films of (a) PBZT (solid line), (b) PBZT/$GaCl_3$ complex (dashed line), (c) PBZT/$AlCl_3$ complex after exposure to air for 3 min (solid line).

Table I. UV–Visible Absorption Data for PBZT and Its Complexes

	λ_{max} (nm)	α_{max} (cm^{-1})[a]	E_g (nm)[b]
PBZT	437	1.55×10^5	491
PBZT/$AlCl_3$ (1:4)	433	1.82×10^5	485
PBZT/$AlCl_3$ hydrate[c]	462	1.52×10^5	551
PBZT/$GaCl_3$ (1:4)	434	1.90×10^5	486
PBZT/$GaCl_3$ hydrate[c]	465	1.50×10^5	550

[a] Absorption coefficient at λ_{max}. [b] Low-energy absorption band edge or optical bandgap. [c] 1:4 complexes exposed to ambient moisture in air for 3 min.

inaccuracy or partial hydration of the complex prior to and during analysis.

Figure 10 shows the UV–visible spectra of films of PBZT (a) and its $AlCl_3$ complex (b). The spectrum obtained after the complex was exposed to ambient moisture in air is shown in Figure 10c. The same series of spectra are shown in Figure 11 for the $GaCl_3$ complex, namely the spectra of PBZT (a), the PBZT/$GaCl_3$ complex (b) and the hydrated complex (c). Absorption data from these spectra are given in Table I. Complexation of PBZT with $AlCl_3$ and $GaCl_3$ (Figures 10b and 11b) results in small blue shifts of the absorption maximum (λ_{max}) and bandgap (E_g), and ~20% increases in the absorption coefficient (α) at the absorption maximum. The increased absorption coefficients on complexation indicate larger transition dipole moments for the complexes than for PBZT. On the other hand, at off-resonant wavelengths (>500 nm) the complexes show much lower absorption coefficients (are more transparent) than pure PBZT. An implication of the increased transition moments in the PBZT com-

plexes is that the off-resonant third-order nonlinear optical susceptibility of the complexes would be larger than the pure PBZT.[9] A similar increase in $\chi^{(3)}$ has been observed in the Lewis acid complexes of other polymers.[28] Furthermore, the smaller absorption coefficients of the complexes relative to PBZT at wavelengths greater than 500 nm suggest that the material figure of merit $\chi^{(3)}/\alpha$ may be enhanced in the complexes.

The hydrated PBZT/$AlCl_3$ and PBZT/$GaCl_3$ complexes (Figures 10c and 11c) exhibit redshifts of λ_{max} and E_g relative to PBZT and its Lewis acid complexes. This is visually evident as a color change from the yellow of the original complexes to the bright red of the hydrated complexes. These hydrated complexes can be viewed as intermediates in the regeneration process between the fully complexed PBZT, and the pure PBZT to which they can be converted by washing with water or another Lewis base. The hydrates are also the same species discussed in relation to the FTIR data which showed that they are essentially decomplexed PBZT containing the metal halide hydrates.

Properties of PBZT Complexes in Solution. In the concentrated solution regime PBZT/$AlCl_3$ and PBZT/$GaCl_3$ complexes exhibit liquid crystallinity with a nematic texture.[16] The critical concentrations (C_{cr}) for anisotropic phase separation are 5 and 8 wt % PBZT in $AlCl_3$/NM and $GaCl_3$/NM, respectively, for the complexes prepared with the stoichiometric Lewis acid in NM. These critical concentrations are significantly higher than a value of 3–4 wt % which was reported for PBZT in MSA.[34] The reason for these higher values lies in the effect of complexation on the axial ratio (molecular length/diameter). Flory[35] has shown that a decrease in axial ratio increases the C_{cr} of a rigid-rod polymer. An approximate relation was given for this dependence:

$$\phi^* = \frac{8}{x}\left(1 - \frac{2}{x}\right) \tag{2}$$

Here ϕ^* is the critical volume fraction of polymer for the appearance of a stable anisotropic phase, i.e., the critical concentration. The parameter x is the axial ratio of the rod molecules. For PBZT we can calculate x using the relation[35]

$$x = \frac{M}{M_u}\frac{l_u}{d} \tag{3}$$

where M is the average molecular weight (29 023), M_u is the repeat unit molecular weight (266.3), l_u is the repeat unit length (12.5 Å[10,36]), and d is the chain diameter, which may be estimated from the equation[35]

$$d = \sqrt{M/\rho N_A l_u} \tag{4}$$

ρ is the polymer density (1.44 g/cm^3 [11,12]) and N_A is Avogadro's number. For PBZT we calculate a chain diameter of 5 Å by using eq 4, an axial ratio of 275 from eq 3 and a ϕ^* of 2.9% by using eq 2. For a comparison of the experimental results with theory we need to convert the measured critical concentrations from weight percent to volume percent. For PBZT in MSA, the reported[34] approximate density is 1.48 g/cm^3. This is very close to that of PBZT and so C_{cr} is 3–4 vol % in this solvent. The densities of nitromethane, $AlCl_3$ and $GaCl_3$ are 1.127, 2.44, and 2.47 g/cm^3, respectively (Aldrich), and from these values we estimate densities of 1.27 and 1.43 g/cm^3 for $AlCl_3$/NM and $GaCl_3$/NM, respectively, at the Lewis acid concentrations used at C_{cr} in each case. The corresponding critical concentrations of PBZT in $AlCl_3$/NM and $GaCl_3$/NM are then 5.6 and 8.0 vol % respectively. The axial ratios can now be calculated. The estimated axial ratio x in MSA (from eq 3) is in the range 198–265 (C_{cr} is 3–4 wt %) and d, calculated by assuming the product xd (molecular length) is constant for all solvents, is 5.1–9.6 Å (from eq 4). For the PBZT/$AlCl_3$ complex in nitromethane, x is predicted to be 141, and d 9.7 Å. The PBZT/$GaCl_3$ complex is predicted to have an axial ratio of 98 and a chain diameter of 13.9 Å.

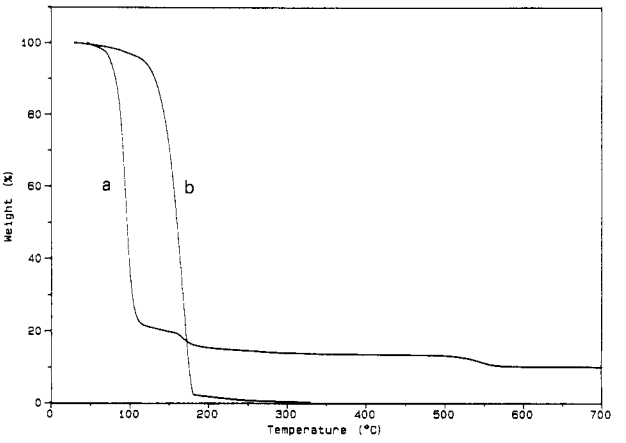

Figure 12. TGA curves of (a) $GaCl_3$ and (b) $AlCl_3$ in flowing nitrogen at 10 °C/min.

These calculations clearly show that Lewis acid complexation reduces the axial ratio for PBZT, apparently more so for $GaCl_3$ complexes than $AlCl_3$ complexes. Thus the coordinated Lewis acid increases the effective molecular diameter of PBZT and thereby decreases the axial ratio and increases C_{cr}.

The absolute viscosity of solutions of PBZT/$AlCl_3$ and PBZT/$GaCl_3$ complexes were reported earlier.[14a] Solutions of PBZT/$AlCl_3$ complexes exhibit a steep increase in viscosity in the concentration range 0–3 wt %. Solutions > 3 wt % PBZT have viscosities >200 Pa S. Solutions > 1 wt % PBZT were found to be shear thinning. Solutions of the PBZT/$GaCl_3$ complex had lower viscosities and were shear thinning at >3 wt % PBZT.

Thermal Properties of Solid Complexes. In Figure 12 are shown the thermogravimetric analysis (TGA) curves of $GaCl_3$ and $AlCl_3$. Figure 12a shows that $GaCl_3$ volatilizes between 85 and 110 °C. Figure 12b shows that $AlCl_3$ is less volatile than $GaCl_3$ and most of the weight loss (>95%) is in the temperature range 100–170 °C. Figure 13a shows the TGA curve for PBZT. The polymer does not exhibit any weight loss below 700 °C. Above ~700 °C the PBZT starts to decompose, losing 23% of its weight by 900 °C. Figure 13b shows the TGA of the PBZT/$AlCl_3$ complex. This complex degrades slowly starting at 100 °C, losing 50% of its weight by 1000 °C. This weight loss is primarily $AlCl_3$ loss since the PBZT structure does not start to degrade until above 700 °C, as shown in Figure 13a. Comparison with Figure 12b shows that volatilization of $AlCl_3$ is retarded in the complex relative to pure $AlCl_3$. This is a result of its coordination to PBZT. $AlCl_3$ constitutes ~67 wt % of the complex and some of this is retained even above 1000 °C. Figure 13c shows the TGA of a PBZT/$AlCl_3$ complex sample which was identical to

(34) Hwang, W. F.; Wiff, D. R.; Benner, C. L.; Helminiak, T. E. *J. Macromol. Sci. Phys. B* **1983**, *22*, 231–257.
(35) Flory, P. J. *Adv. Polym. Sci.* **1984**, *59*, 1–35.

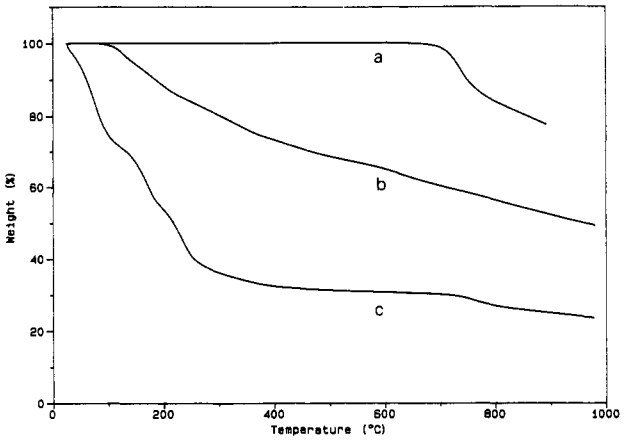

Figure 13. TGA curves of (a) PBZT, (b) 1:4 PBZT:$AlCl_3$ cast from NM, and (c) the complex of (b) after exposure to air for a few minutes, in flowing nitrogen at 10 °C/min.

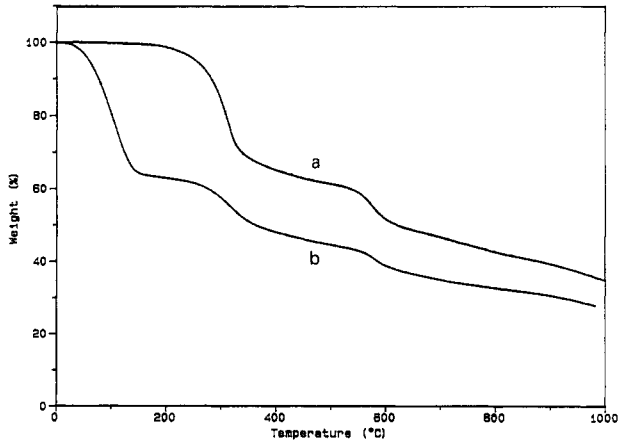

Figure 14. TGA curves of (a) 1:4 PBZT:$GaCl_3$ cast from NM (b) complex of (a) after exposure to air for several minutes, in flowing nitrogen at 10 °C/min.

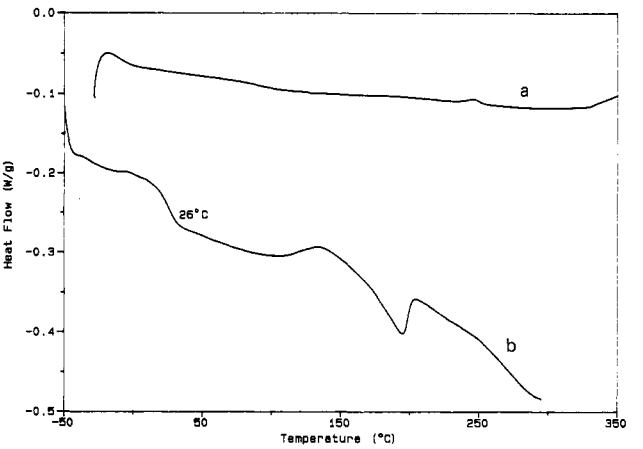

Figure 15. DSC thermograms of (a) PBZT and (b) PBZT/$GaCl_3$ complex prepared as in Figure 14a. The heating rate was 20 °C/min.

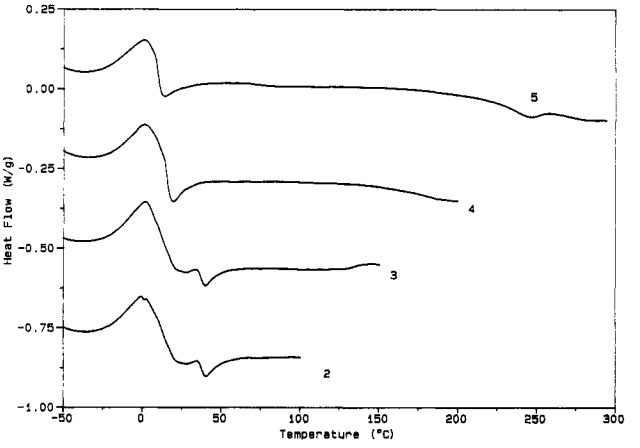

Figure 16. Successive DSC thermograms of 1:4 PBZT:$GaCl_3$ complex prepared in dichloromethane. Run 1 which is not included showed a large endotherm peaking at ~38 °C due to evaporation of dichloromethane. The heating rate was 20 °C/min.

that of Figure 13b and was exposed to ambient moisture in air for several minutes prior to running the TGA experiment. The data demonstrate the moisture sensitivity of the complex. Most of the initial weight loss is due to the metal halide hydrate.

The TGA curve of the PBZT/$GaCl_3$ complex is shown in Figure 14a. By comparison with Figure 13b, this complex is significantly more stable than the PBZT/$AlCl_3$ complex, since it exhibits no weight loss below ~200 °C. The subsequent weight loss is primarily $GaCl_3$ retarded in its evolution from the sample, compared to the pure $GaCl_3$ in Figure 12a, because of its coordination to PBZT. More quantitatively, at 900 °C the complex has lost ~65% of its weight. The complex is made up of about 27.5 wt % PBZT and 72.5 wt % $GaCl_3$ (4:1 $GaCl_3$:PBZT stoichiometry). If we assume that the PBZT portion of this complex degrades exactly as pure PBZT degrades (Figure 13a), only 6% of this 65% weight loss is due to PBZT degradation. The remaining 59% is then due to loss of $GaCl_3$. This implies that at 900 °C, only 81% of the $GaCl_3$ present in the original complex has evolved from the sample. The rest is coordinated to the PBZT residue even at this high temperature. Figure 14b shows the TGA of the PBZT/$GaCl_3$ complex after exposure to ambient moisture in air for several minutes. The data demonstrate that the complex is very sensitive to moisture as evidenced by the large initial weight loss due to the metal halide hydrate. The PBZT/BCl_3 complexes exhibited significant weight losses at room temperature and were therefore considered thermally unstable.

Differential scanning calorimetry (DSC) of PBZT did not reveal any glass transition or melting point for the polymer, as shown in Figure 15a, and none are known to exist below the decomposition temperature.[5] The apparent small peak at ~250 °C in Figure 15a is due to baseline irregularity as confirmed by its presence in a similar DSC scan of an empty DSC pan. The DSC thermogram of the 4:1 $AlCl_3$:PBZT complex (not shown) showed no discernible transitions below decomposition which starts just above ~100 °C (as discussed in relation to Figure 13b). On the other hand the DSC thermogram of the 4:1 $GaCl_3$:PBZT complex which is more thermally stable, as discussed earlier, could be obtained up to 175–200 °C without significant decomposition. Figure 15b shows the DSC scan of the PBZT/$GaCl_3$ complex prepared from a nitromethane solution. Strikingly, the complex shows a glass transition with onset at 18 °C, endpoint at 31 °C and a midpoint (T_g) of 26 °C. This T_g could be reproduced in repeated scans below ~175 °C.

Figure 16 shows successive DSC scan of a sample of the 4:1 $GaCl_3$:PBZT complex prepared in dichloromethane. The numbers labeling the scans indicate the chronological order in which they were obtained. In run 1, which is not shown, the glass transition was enveloped by a large

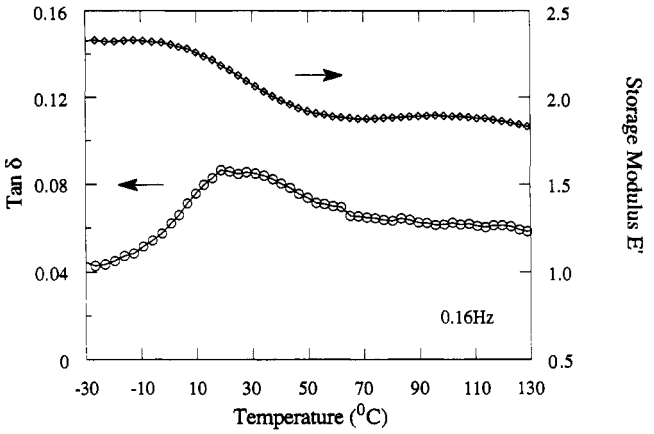

Figure 17. Temperature-dependent loss tangent (tan δ) and storage modulus (E') of the PBZT/$GaCl_3$ complex obtained at a frequency of 0.16 Hz. The complex was that shown in Figure 14a. The units of E' are relative since the samples were sandwiched between glass plates.

Table II. Dynamic Mechanical Analysis Data for the 4:1 $GaCl_3$:PBZT Complex.

frequency (Hz)	T_δ (°C)[a]	$T_{onset,E'}$ (°C)[b]
0.16	24	6
1.6	37	18
15.0	50	31

[a] Glass transition temperature measured as the maximum in a plot of loss tangent vs temperature. [b] Temperature of onset of decrease in the storage modulus (E') in a plot of E' vs temperature.

endotherm peaking at 38 °C which was due to evaporation of residual DCM in the sample. The sample was heated to 50 °C during run 1. In run 2 the glass transition appears at about 13 °C along with a small endotherm at 38 °C due to remaining dichloromethane. Run 3 is almost identical to run 2. Heating of the sample to 150 °C during run 3 results in complete disappearance of the 38 °C peak in runs 4 and 5 and the T_g shifts to about 16 °C. This is lower by 10 °C than the T_g observed in Figure 15b for the PBZT/$GaCl_3$ complex prepared from a nitromethane solution. This difference is due to the broadness of the transition (13 °C in Figure 15b) and the experimental variability between samples.

The glass transition of the PBZT/$GaCl_3$ complex prepared from nitromethane was investigated further by dynamic mechanical analysis (DMA). Figure 17 shows plots of the temperature dependent storage modulus (E') and loss tangent (tan δ) of a PBZT/$GaCl_3$ complex at a frequency of 0.16 Hz. The plots show the characteristic step change in E' and a tan δ peak which accompany a glass transition.[37] Similar experiments at 1.6 and 15 Hz also revealed a step change in E' and tan δ peak. The temperatures of onset of the decrease in E' and the maximum in tan δ are presented in Table II for all three frequencies. T_δ is normally considered to be the glass transition temperature at a given frequency. At the lowest frequency (0.16 Hz) the observed (peak value) T_δ of 24 °C is close to the 26 °C (midpoint value) observed by DSC. As expected, the glass transition is an activated process and Figure 18 shows Arrhenius plots of the frequency dependence of the onset of decrease of E' and T_δ. From

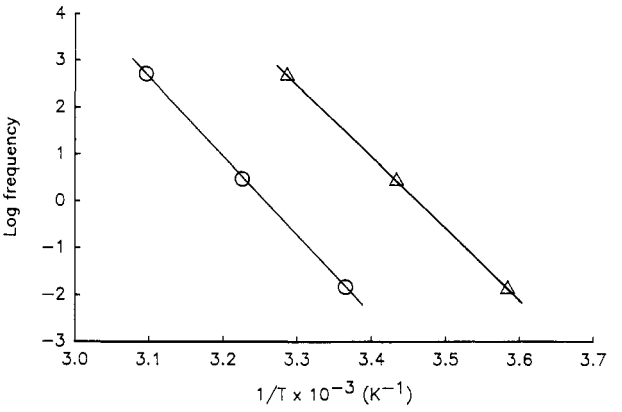

Figure 18. Inverse temperature ($1/T$) vs natural logarithm of frequency for the maximum in tan δ temperature (circles) and onset temperature of the decrease in E' (triangles) for the PBZT/$GaCl_3$ complex.

these plots we obtain an activation energy of 32 kcal/mol for the transition of the PBZT/$GaCl_3$ complex. The magnitude of this value gives us some insight into the nature of the transition process. This energy is higher than for flexible chain polymers due to the rigidity of PBZT chains. For example, the β-transition of poly(cyclohexyl methacrylate) is reported to exhibit an activation energy of 11.5 kcal/mol (page 23 in ref 37). On the other hand, it is much lower than for some semirigid chain polymers which exhibit glass transitions (e.g., amorphous poly(ethylene terephthalate) the glass transition of which has an activation energy of 184 kcal/mol (page 505 in ref 37)). The significantly smaller activation energy for the glass transition of the complex is due to the greatly reduced intermolecular interactions in the complex compared to pure PBZT.

The observed dramatic reduction of the glass transition temperature of PBZT on Lewis acid complexation is in accord with our observation of the effect of complexation on both rigid-chain and flexible-chain polymers with strong intermolecular interactions.[38] The decrease of T_g on complexation sheds light on the critical role of intermolecular forces on the value of the glass transition temperature. A practical implication of this result in the case of PBZT is that it may be possible to devise novel "melt" processing approaches for the polymer.

Conclusions

We find that the complexes of PBZT are characterized by coordinate covalent bonding of the Lewis acids to the heteroatoms. Solubilization of PBZT in nitromethane requires a 4:1 Lewis acid:PBZT repeat unit stoichiometry. This amount of Lewis acid coordinates to the polymer (i.e., 4 mol/repeat unit) forming electron donor–acceptor complexes in which the metal atoms of the Lewis acid are coordinated to the nitrogen and sulfur heteroatoms of PBZT. The aluminum atoms are tetrahedral in these complexes and withdrawal of the lone pair electrons causes a rehybridization within the PBZT structure.

Coordination of the Lewis acids to PBZT increases the average molecular diameter of the polymer chains which decreases the axial ratio. This is manifested experimentally by higher critical concentrations for anisotropic phase

(36) Fratini, A. V.; Lenhert, P. G.; Resch, T. J.; Adams, W. W. *Mater. Res. Soc. Symp. Proc.* **1989**, *134*, 431–445.

(37) McCrum, N. G.; Read, B. E.; Williams, G. *Anelastic and Dielectric Effects in Polymer Solids*; Dover Publications: New York, 1991; pp 43–56.

(38) (a) Roberts, M. F.; Jenekhe, S. A. *Mater. Res. Soc. Symp. Proc.* **1991**, *215*, 23–28. (b) Jenekhe, S. A.; Roberts, M. F. *Macromolecules* **1993**, *26*, 4981–4983.

separation in solutions of the PBZT complexes compared to protonated PBZT. The pure liquid crystalline solutions of PBZT/Lewis acid complexes should be useful for preparing oriented forms of PBZT. The higher critical concentrations and ease of processing from organic solvents offer significant improvements in processability compared to conventional acid processing of PBZT.[2,4]

Our observation of the glass transition of the PBZT/$GaCl_3$ complex at about 26 °C is particularly significant in light of the fact that the T_g of PBZT is greater than 650 °C. The relatively low T_g value of the complex is the result of substantially reduced intermolecular attractive forces on complexation, the same phenomenon which accounts for the solubility in organic solvents. One practical implication is that it may be possible to "melt" process PBZT through its low T_g complex.

The complexes were found to maintain the rigid-rod conformation and π-conjugation characteristics of PBZT. The increased transition dipole moments in the PBZT/Lewis acid complexes compared to PBZT, as evidenced by the increased absorption coefficients of the lowest energy absorption band, have the interesting implication that the third order nonlinear optical susceptibility ($\chi^{(3)}$) of the complexes would also be larger at off resonant wavelengths.[9,28] Furthermore the low absorption coefficients of the complexes compared to PBZT at off-resonant wavelengths (>500 nm) suggest that the figure of merit ($\chi^{(3)}/\alpha$) of heterocyclic nonlinear optical polymers might be improved by complexation.

Acknowledgment. We thank John Osaheni of our laboratory for synthesis of the PBZT sample and assistance in obtaining the fluorescence spectra. The t-DBZT sample provided to us by the Air Force Materials Laboratory is also appreciated. This research was supported in part by the Amoco Foundation, the NSF Center for Photoinduced Charge Transfer and an Elon Huntington Hooker Fellowship to MFR.